Objective evaluation of prediction strategies for optimization-based motion cueing

Grottoli, Marco; Cleij, Diane; Pretto, Paolo; Lemmens, Yves; Happee, Riender; Bülthoff, Heinrich H.

DOI
10.1177/0037549718815972

Publication date
2019

Document Version
Final published version

Published in
Simulation

Simulation

Applications

Simulation: Transactions of the Society for Modeling and Simulation International
1–18


DOI: 10.1177/0037549718815972
journals.sagepub.com/home/sim
SAGE SCS

Objective evaluation of prediction strategies for optimization-based motion cueing

Marco Grottoli[1,2], Diane Cleij[1,3], Paolo Pretto[3,4], Yves Lemmens[2], Riender Happee[1] and Heinrich H. Bülthoff[3]

Abstract

Optimization-based motion cueing algorithms based on model predictive control have been recently implemented to reproduce the motion of a car within the limited workspace of a driving simulator. These algorithms require a reference of the future vehicle motion to compute a prediction of the system response. Assumptions regarding the future reference signals must be made in order to develop effective prediction strategies. However, it remains unclear how the prediction of future vehicle dynamics influences the quality of the motion cueing. In this study two prediction strategies are considered. *Oracle*: the ideal prediction strategy that knows exactly what the future reference is going to be. *Constant*: a prediction strategy that ignores every future change and keeps the current vehicle's linear accelerations and angular velocities constant. The two prediction strategies are used to reproduce a sequence of maneuvers between 0 and 50 km/h. A comparative analysis is carried out to objectively evaluate the influence of the prediction strategies on motion cueing quality. Dedicated indicators of correlation, delay and absolute error are used to compare the effects of the adopted prediction on simulator motion. Also the motion cueing mechanisms adopted by the different conditions are analyzed, together with the usage of simulator workspace. While the constant strategy provided reasonable cueing quality, the results show that knowledge of the future vehicle trajectory reduces the delay and improves correlation with the reference trajectory, it allows the combined usage of different motion cueing mechanisms and increases the usage of workspace.

Keywords

Driving, simulation, motion, cueing, prediction.

1. Introduction

Motion cueing algorithms (MCAs) are used in driving simulators to provide inertial motion to the user of the simulator. The motion obtained from the vehicle dynamic simulation is adjusted by the MCA to fit the limited workspace of the simulator motion system. To achieve this goal, different algorithms have been developed in the past decades. One of the most commonly used MCAs is known as the classical algorithm.[1–3] Classical MCAs are based on filters, where linear accelerations and angular velocities are first scaled and then high-pass filtered to remove constant signal content (washout). In addition, low-pass filters are also used for longitudinal and lateral accelerations, where tilt coordination is adopted to use gravitational acceleration to reproduce sustained accelerations. These algorithms present some limitations. The tuning process is not trivial and it is often subjective. Different approaches have been studied to objectively tune the parameters of classical MCAs by following a specific process[4] or by optimizing a set of dedicated objective metrics of motion cueing quality.[5,6] Nevertheless, the results obtained from these techniques can still be improved by further subjective tuning. The tuning process of classical MCAs is specific to the set of maneuvers to reproduce on the motion simulator. Since classical MCAs do not include knowledge of the motion system's limitation, the tuning process must

[1]Delft University of Technology, The Netherlands
[2]Siemens PLM Software, Leuven, Belgium
[3]Max Planck Institute for Biological Cybernetics, Tübingen, Germany
[4]Virtual Vehicle Research Center, Graz, Austria

Corresponding author:
Marco Grottoli, Delft University of Technology, Faculty of 3mE (BMechE), Mekelweg 2, 2628 CD Delft, The Netherlands.
Email: m.grottoli@tudelft.nl

be repeated if the set of maneuvers changes. Otherwise, the trajectory obtained by the classical MCA could be exceeding the physical boundaries of the motion system. More recently another approach based on optimization has become popular.[7–10] Unlike filter-based MCAs, the optimization-based approach uses model predictive control (MPC) to compute an optimal solution, within system limitations, using an internal model of the motion system to predict the future system response.[11–14] This algorithm will be referred to here as 'predictive MCA'. This new approach takes into account motion system limitations and the tuning is achieved with weighting factors on linear and rotational motion cues. The predictive MCA has shown multiple advantages with respect to the classical algorithm, both in terms of workspace usage and subjective evaluation, when the vehicle trajectory is completely known in advance (passive driving).[15] However, other challenges are introduced with the usage of predictive MCA. Compared with the classical MCA, this algorithm requires more computational time to solve an optimization problem at each time step of the algorithm, making it more challenging to adopt for more common driver-in-the-loop (DIL) simulations (active driving). Another aspect to consider is that the predictive MCA requires a future reference of the motion to reproduce on the simulator to compute a prediction of the system response. When using the predictive MCA in DIL simulations, assumptions regarding the future reference signals must be made. Previous studies have already addressed the issue of providing a future reference for the predictive MCA. For example, the vehicle motion recorded in a circuit is used to provide a better reference for future laps,[16] or a neural network is trained using simulated data to predict the future reference motion.[17] However, it remains unclear how the prediction strategies adopted influence the quality of the motion cueing. In this study, two prediction strategies are considered. The first strategy corresponds to the ideal case in which the future motion to be reproduced on the simulator is known, as if it could be perfectly predicted. This cannot be applied for active driving but represents the perfect strategy which is expected to reproduce, at best, the reference motion and therefore it is assumed here as a reference. The second strategy assumes a constant motion as a future reference, ignoring every possible variation from the current status. It can be expected that the results for this strategy will be suboptimal with respect to the first one. The scenario used to compare the results of the two prediction strategies is the reproduction on a motion-based simulator of a sequence of maneuvers in an urban-like environment. The simulations are performed offline and the future reference for the few seconds ahead is passed to the predictive MCA at each time step, as if it would be for a DIL simulation. The simulator motion computed with the considered prediction strategies is analyzed and compared with the reference motion.

The goal of this study is to objectively evaluate the influence of the adopted prediction strategy on motion cueing quality. The analysis carried out should also determine whether it is worth investing in an improved prediction strategy to obtain a better motion cueing quality.

2. Methods

2.1. Motion perception

The main role of the MCA is to reproduce the simulated vehicle motion as accurately as possible for the simulator user. In the process of motion perception, humans use visual, vestibular and proprioceptive organs to detect motion direction and rate of change. The vestibular system is located in the inner ear and consists of semicircular canals and otolith organs, which sense angular and linear motion respectively. More specifically, the otolith organs detect specific forces, which result from summation of acceleration in space and gravity. Thus, the specific forces ($\mathbf{f}$) can be expressed as follows, where $\mathbf{a_{ng}}$ indicates the non-gravitational accelerations and $\mathbf{g}$ indicates the gravitational acceleration:

$$\mathbf{f} = \mathbf{a_{ng}} - \mathbf{g} \tag{1}$$

Therefore, humans are unable to discriminate between linear accelerations and the component of gravitational acceleration that occurs when the head is tilted with respect to the gravity vector.[1] This effect can be exploited in motion simulators, allowing to reproduce sustained accelerations by simulator tilt. The use of tilt angles is limited to 20–30 deg (Aubert effect), which limits the maximum possible acceleration simulated via tilt coordination to 0.5 g.[18] The use of tilt coordination generates additional motion in the rotational channels, and in order for this false motion not to be noticed, the tilt rate should be limited to the angular velocity perception threshold. Different values of this threshold can be found in literature; a unique value is difficult to identify given also the subjective nature and the dependency from the simulation scenario (active/passive driving). In this study a value of 3 deg/s is considered.[19,20] Humans require additional sensory information (i.e., visual, proprioceptive) in order to discriminate between acceleration and tilt.[21]

A vestibular system model is not considered here. In this study the goal of the MCA is to reproduce, on the motion simulator, the specific forces and the angular velocities obtained from a vehicle dynamics simulation. The predictive MCA computes the optimal simulator motion and predicts the associated perceived motion of the driver on the simulator. Vehicle-specific forces and angular velocities are used as a reference motion for the predictive MCA in order to minimize the difference between the motion on the simulator and in the real vehicle.

Table 1. Maximum longitudinal acceleration (a_x), lateral acceleration (a_y), maximum yaw rate (ω_z) and maximum significant frequency content of the considered vehicle maneuvers.

Maneuver	$a_x[m/s^2]$	$a_y[m/s^2]$	$\omega_z[deg/s]$	$[Hz]$
A	2	–	–	0.4
B	3	–	–	0.4
CT	–	2	10	0.2
DLC	–	± 1	± 5	0.3
BCTA	± 1	2	10	0.2

A: accelerating; B: braking; BCTA: braking while entering the turn and accelerating while exiting the turn; CT: constant turn; DLC: double lane change.

2.2. Vehicle maneuvers

The maneuvers to reproduce on the motion-based simulators are selected in an urban-like scenario between 0 and 50 km/h. The simulated vehicle performs the following maneuvers:

- A: accelerating from 0 to 50 km/h
- B: braking from 50 to 0 km/h
- CT: constant turn at 50 km/h
- DLC: double lane change at 50 km/h
- BCTA: braking from 50 to 30 km/h while entering the turn and accelerating from 30 to 50 km/h while exiting the turn

The maneuvers have been selected to explore typical longitudinal, lateral and combined motion scenarios. In particular A and B are purely longitudinal maneuvers, while CT and DLC are purely lateral. In addition, BCTA has been chosen to evaluate the combined longitudinal and lateral dynamics. A description of these maneuvers in terms of maximum accelerations and significant frequency content is given in Table 1. The frequency spectrum of the vehicle motion is computed and the maximum significant frequency of each maneuver is considered as the frequency above which the amplitude of the signal's spectrum is below 10% of its maximum. The vehicle dynamic simulations have been performed with a time step of 1 ms using CarSim™ (Mechanical Simulation Corporation, Ann Arbor, MI, United States). The selected vehicle was a mid-size sedan and it was autonomously driven over a predefined path at a controlled speed. The simulation was performed offline and the results have been filtered to remove the high frequency content of the vehicle motion using a zero-phase low-pass 4th-order Butterworth filter with cut-off frequency of 12.6 rad/s.

2.3. Predictive MCA

The MCA adopted in this study is based on MPC. This advanced control technique uses a simplified model of the system under control (i.e., motion system used in dynamic simulators, to predict the future system's response and optimize the control action to achieve optimal tracking performances within system limitations). The motion system considered for this study is a six degrees of freedom (DOF) hexapod[22] with a linear actuator stroke of 0.533 m and resulting single DOF limits reported in Table 2.

Table 2. Motion system single DOF limits.

DOF	Position		Velocity	Acceleration
x	$-0.423\ m$	$0.540\ m$	$\pm\ 0.8\ m/s$	$\pm\ 7\ m/s^2$
y	$-0.432\ m$	$0.432\ m$	$\pm\ 0.8\ m/s$	$\pm\ 7\ m/s^2$
z	$-0.306\ m$	$0.324\ m$	$\pm\ 0.55\ m/s$	$\pm\ 10\ m/s^2$
Roll	$-20.25\ deg$	$20.25\ deg$	$\pm\ 33.5\ deg/s$	$\pm\ 245\ deg/s^2$
Pitch	$-23.85\ deg$	$20.70\ deg$	$\pm\ 36.5\ deg/s$	$\pm\ 245\ deg/s^2$
Yaw	$-23.40\ deg$	$23.40\ deg$	$\pm\ 39.5\ deg/s$	$\pm\ 498\ deg/s^2$

DOF: degrees of freedom.

In order to define the equations of motion of the considered motion system, the following frames of reference are defined:

- Inertial frame (IF): fixed to the ground and placed at the center of the hexapod fixed base
- Platform frame (PF): placed at the center of the hexapod moving base
- Head frame (HF): positioned at the head center of the simulator user

The non-linear equations of motion of the system have been derived, considering the moving platform as a single rigid body with mass, m, and inertia tensor, $\mathbf{I}$. The rigid body is subject to three orthogonal forces ($\mathbf{F}$) and three orthogonal torques ($\mathbf{M}$) applied at the center of mass. The complete equations of motion are as follows:

$$\begin{cases} \dot{\mathbf{p}} = \mathbf{v} \\ \dot{\mathbf{q}} = \dfrac{1}{2} E^T \boldsymbol{\omega} \\ \dot{\mathbf{v}} = \dfrac{\mathbf{F}}{m} + \mathbf{g} \\ \dot{\boldsymbol{\omega}} = \mathbf{I}^{-1}(\mathbf{M} - \boldsymbol{\omega} \times \mathbf{I}\boldsymbol{\omega}) \end{cases} \tag{2}$$

with,

$$E = \begin{bmatrix} -q_1 & q_0 & q_3 & -q_2 \\ -q_2 & -q_3 & q_0 & q_1 \\ -q_3 & q_2 & -q_1 & q_0 \end{bmatrix} \tag{3}$$

where, $\mathbf{p}$ and $\mathbf{v}$ are respectively the position and the velocity of the center of mass expressed in IF, $\mathbf{q}$ is the vector of the orientation quaternions and $\boldsymbol{\omega}$ the rotational velocity vector expressed in PF.

In order to proceed to the full problem statement, the state vector $\mathbf{x}$ and the input vector $\mathbf{u}$ of the controlled system are defined as follows:

$$\mathbf{x} = \begin{bmatrix} \mathbf{p} \\ \mathbf{q} \\ \mathbf{v} \\ \boldsymbol{\omega} \end{bmatrix} \quad \mathbf{u} = \begin{bmatrix} \mathbf{F} \\ \mathbf{M} \end{bmatrix} \tag{4}$$

The system is also subject to constraints, and the MPC allows their inclusion in the optimization problem. As a result, the computed motion trajectory will be optimized while still remaining within system limitations.

The main physical constraint comes from the system's actuators, which are limited within a certain range of motion. This limitation is expressed as an inequality constraint, where the actuator length is bounded between minimum ($\mathbf{L}_{\min}$) and maximum values ($\mathbf{L}_{\max}$). The lengths of the actuators can be computed solving the hexapod inverse kinematics,[23] as follows:

$$\mathbf{L}_i = \|\mathbf{R}(\mathbf{q})\,\mathbf{T}_i + \mathbf{p} - \mathbf{B}_i\| \qquad \text{for } i = 1, \ldots, 6 \tag{5}$$

where, $\mathbf{L}_i$ is the length of the i_{th} actuator, $\mathbf{T}_i$ and $\mathbf{B}_i$ are the coordinate vectors of the actuator's mounting points on the moving and fixed base respectively. The expression is non-linear due to the presence of the rotation matrix $\mathbf{R}(\mathbf{q})$ as follows:

$$\mathbf{R}(\mathbf{q}) = \begin{bmatrix} 1-2q_2^2-2q_3^2 & 2(q_1q_2-q_0q_3) & 2(q_1q_3+q_0q_2) \\ 2(q_1q_2+q_0q_3) & 1-2q_1^2-2q_3^2 & 2(q_2q_3-q_0q_1) \\ 2(q_1q_3-q_0q_2) & 2(q_2q_3+q_0q_1) & 1-2q_1^2-2q_2^2 \end{bmatrix} \tag{6}$$

The constraint (Equation 5) is linearized with respect to the state vector as follows:

$$\mathbf{L} \approx \mathbf{M}_k\mathbf{x}_k + \mathbf{Q}_k \tag{7}$$

where, $\mathbf{M}_k$ is the Jacobian matrix of the vector $\mathbf{L}$ with respect to the state vector $\mathbf{x}_k$, and $\mathbf{Q}_k$ is the constant term of the linear approximation. Both $\mathbf{M}_k$ and $\mathbf{Q}_k$ are updated at each time step using the current state vector $\mathbf{x}_k$ and included in the optimal control problem formulation.

Together with the actuators' length constraint, the single DOF motion limitation has also been included in the optimization problem. This constraint somewhat reduces the usable platform workspace, but was considered anyway for extreme caution.

As introduced in Section 2.1, vehicle linear accelerations and angular velocities are considered as the target reference for the MPC controller. The aim of the controller is to reproduce the perceived motion as would occur in the real vehicle, but keeping the simulator motion within its physical limitations. The output function expresses the perceived motion in terms of specific forces ($\mathbf{f}$) and angular velocities (ω) on the simulator in HF, where the frame is indicated in the quantity subscription. The relevant quantities are first written in PF, where also the angular acceleration vector α is defined as follows:

$$\begin{aligned} \mathbf{f}_{PF}(\mathbf{x},\mathbf{u}) &= \mathbf{R}^T(\mathbf{g} - \dot{\mathbf{v}}) \\ \boldsymbol{\omega}_{PF}(\mathbf{x}) &= \boldsymbol{\omega} \\ \boldsymbol{\alpha}_{PF}(\mathbf{x},\mathbf{u}) &= \dot{\boldsymbol{\omega}} \end{aligned} \tag{8}$$

Next, the same quantities can be expressed in HF by means of the rotation matrix from PF to HF (${}^{HF}\mathbf{R}_{PF}$) and the translation vector from HF to PF (${}^{PF}\mathbf{r}_{HF}$). The definition of the output quantities in HF is as follows:

$$\begin{aligned} &\mathbf{f}_{HF}(\mathbf{x},\mathbf{u}) = {}^{HF}\mathbf{R}_{PF}[\mathbf{f}_{PF}(\mathbf{x},\mathbf{u}) + \\ &-\boldsymbol{\alpha}_{PF}(\mathbf{x},\mathbf{u}) \times {}^{PF}\mathbf{r}_{HF} - \boldsymbol{\omega}(\mathbf{x}) \times (\boldsymbol{\omega}(\mathbf{x}) \times {}^{PF}\mathbf{r}_{HF})] \\ &\boldsymbol{\omega}_{HF}(\mathbf{x}) = {}^{HF}\mathbf{R}_{PF}\boldsymbol{\omega}_{PF}(\mathbf{x}) \end{aligned} \tag{9}$$

As a result, the system output vector $\mathbf{y}$ is defined in vector form as follows:

$$\mathbf{y}(\mathbf{x},\mathbf{u}) = \begin{bmatrix} \mathbf{f}_{HF}(\mathbf{x},\mathbf{u}) \\ \boldsymbol{\omega}_{HF}(\mathbf{x}) \end{bmatrix} \tag{10}$$

The system's equations of motion and output equations are then discretized and converted to a discrete time dynamic model using the direct multiple shooting method.[24]

The complete non-linear constrained optimization problem is formulated as follows:

$$\begin{aligned} \underset{\substack{\mathbf{u}_0,\mathbf{u}_1,\ldots,\mathbf{u}_{N-1} \\ \mathbf{x}_0,\mathbf{x}_1,\ldots,\mathbf{x}_N}}{\text{minimize}} \quad & \sum_{k=0}^{N-1} I_k(\mathbf{x}_k,\mathbf{u}_k) + I_N(\mathbf{x}_N) \\ \text{subject to } & \mathbf{x}_0 = \tilde{\mathbf{x}}_0 \\ & \mathbf{x}_{k+1} = A_k\mathbf{x}_k + B_k\mathbf{u}_k \\ & \mathbf{x}_{\min} \leqslant \mathbf{x}_k \leqslant \mathbf{x}_{\max} \\ & \mathbf{L}_{\min} \leqslant \mathbf{M}_k\mathbf{x}_k + \mathbf{Q}_k \leqslant \mathbf{L}_{\max} \\ & \mathbf{x}_{\min,N} \leqslant \mathbf{x}_N \leqslant \mathbf{x}_{\max,N} \\ & \mathbf{u}_{\min} \leqslant \mathbf{u}_k \leqslant \mathbf{u}_{\max} \end{aligned} \tag{11}$$

With $k = 0, \ldots, N-1$. Where,

$$\begin{aligned} I_k(\mathbf{x}_k,\mathbf{u}_k) &= \|\hat{\mathbf{y}}_k - \mathbf{y}(\mathbf{x}_k,\mathbf{u}_k)\|^2_{W_y} + \|\hat{\mathbf{x}}_k - \mathbf{x}_k\|^2_{W_x} + \\ &+ \|\hat{\mathbf{u}}_k - \mathbf{u}_k\|^2_{W_u} \\ I_N(\mathbf{x}_N) &= \|\hat{\mathbf{x}}_N - \mathbf{x}_N\|^2_{W_{x_N}} \end{aligned} \tag{12}$$

The MPC controller solves this problem at each time step. The implementation has been done in Matlab (The MathWorks, Inc., Natick, MA, United States) and the quadratic programming problem is solved by a separate solver (qpOASES[25]).

The optimization problem in Equation 11 is defined to minimize the cost function expressed by the two terms I_k and I_N, defined in Equation 12. The term I_k of the cost function is defined as a sum of weighted squared norms of

the difference between the vector quantities and their references over the prediction horizon of N time steps from 0 to $N-1$, while the term I_N includes only the final state cost expressed as a weighted squared norm of the difference between the final state vector and its reference. Both terms include the reference values which are defined over the prediction horizon before to solve the optimization problem. These references are: $\hat{\mathbf{y}}_k$, $\hat{\mathbf{x}}_k$, $\hat{\mathbf{u}}_k$ and $\hat{\mathbf{x}}_N$, which represent the reference trajectory for system output, state, input and final state respectively. The inclusion of these terms in the cost function has different meanings. For instance, by giving a null reference to the state over the prediction horizon a behavior similar to a washout filter would be obtained, where the MCA tries to keep the hexapod in its central position. For this study, this effect will not be considered and therefore the reference state $\hat{\mathbf{x}}_k$, as well as the respective weights W_x, will be set to zero. The addition of a null reference for input and final state in the cost function stabilizes the system. The stabilization effects are controlled by setting the associated weights. In this study, the references for both $\hat{\mathbf{u}}_k$ and $\hat{\mathbf{x}}_N$ are set to zero over the prediction horizon. The weights on the input are $1e^{-3}$ for the linear accelerations and $1e^{-1}$ for the angular velocities, while the weights on the final states are $1e^{1}$ for all the states. The remaining term is the reference trajectory for the system output $\hat{\mathbf{y}}_k$, which needs to be defined at each time step in order to optimize the control action. The definition of the output reference is not only necessary to numerically solve the control problem, but the accuracy of future reference will also affect the performances of the algorithm. For example, if the reference includes changes derived from a particular maneuver to reproduce on the simulator, the algorithm will know it in advance and it will make use of this knowledge to improve the results. The output reference is defined by the prediction strategy. In this study, two different prediction strategies were compared: *oracle* and *constant*.

2.3.1 Prediction strategies. The first prediction strategy considered for this study is the ideal strategy that is able to predict with perfect accuracy the future vehicle motion. This strategy will be referred to here with the name *oracle* (due to its 'prophetic' capabilities in predicting the future[26]). Clearly, this strategy cannot be adopted in an active driving simulation but it is considered as a reference to evaluate the best possible motion cueing quality achievable with the predictive MCA. In order to implement the *oracle* strategy, linear accelerations and angular velocities resulting from the vehicle dynamic simulations must be known a priori. At each time step, and for the length of the prediction horizon, the corresponding signals are extracted from the fully known motion and provided to the predictive MCA.

The second strategy adopted in this study does not consider any assumptions on future vehicle behavior and, at each time steps, simply holds the current value of linear accelerations and angular velocities that results from the vehicle simulation. This strategy will be referred to here as *constant*. Contrary to the *oracle*, this strategy can be adopted for active driving simulation, but the resulting motion cueing quality is expected to be lower.

2.3.2 Prediction horizon length. An important aspect of the future prediction is given by the length of the prediction horizon. The further the algorithm can see in the future, the sooner it will respond to a future change. On the other hand, a longer prediction horizon would result in a very high computational cost. In a previous study[27] a genetic algorithm was adopted to optimize the length of the control and prediction horizon of the MPC. In another study[28] a model was developed to evaluate the relation between prediction horizon length and performance of the predictive MCA in terms of a reduction of cost function. In the last study, the cost value obtained with a certain prediction length $c(h)$ was compared with the cost obtained with an infinite prediction c_∞. A parametric model was developed and it is reported here as follows:

$$\frac{c(h)}{c_\infty} - 1 = \left(\frac{h}{a}\right)^{-k} \tag{13}$$

Where a and k are characteristic parameters depending on the considered scenario. The results showed that for an urban-like scenario the characteristic time a for which the cost is twice the value with infinite horizon is 3.3 seconds and the cost decrease factor k is equal to 2. In this study a prediction horizon of 5 seconds is considered, which is roughly 1.5 times the characteristic time and would result in a cost value of approximately 1.4 times the cost with infinite horizon. The choice of 5 seconds of prediction, together with the selected time step of 0.1 seconds, results in an horizon length, N, equal to 50 and a total number of control parameters to optimize equal to 300. The implementation adopted in this study does not allow real time performances for a problem of this size. In order to improve the performance to real-time, a different implementation could be adopted using more efficient programming language and/or optimization algorithm.

2.3.3 Weighting factor optimization. The motion cueing quality that can be achieved with the predictive MCA depends on the accuracy of the predicted motion that is provided to the MPC algorithm at each time step. The MPC algorithm aims at reproducing the given reference signals where the tracking performances are influenced by the weighting factors associated with each motion channel.

Table 3. Initial and optimized weighting factors on specific forces and angular velocities of the predictive MCA.

Weight	Specific forces			Angular velocities		
	f_x	f_y	f_z	ω_x	ω_y	ω_z
Oracle						
Initial	1	1	1	100	100	100
Optimal	3.021	1.101	3.031	100.310	101.239	100.574
Constant						
Initial	1	1	1	100	100	100
Optimal	1.000	1.579	1.579	100.013	100.000	100.000

MCA: Motion cueing algorithm.

In the considered problem formulation, the weighting factors associated with the perceived motion are the six non-zero terms of the diagonal matrix W_y. Finding the optimal values of these weights is not trivial and it can strongly influence the results of the predictive MCA. Using the same set of weights for both prediction strategies might be unfair for the comparison of the obtained motion cueing results. Therefore an optimization of the weights is performed with the aim of finding the best possible set for each prediction strategy. The weights are initialized with values taken from literature[28,15] and reported in Table 3, where the different order of magnitude is to account for the ratio between specific forces (in m/s^2) and angular velocities (in rad/s) for typical maneuvers.[28] The simulator motion obtained with *oracle* and *constant* strategies for the entire sequence of maneuvers is used to compute the error with respect to the vehicle motion. The error is computed separately for linear (e_f) and rotational motion (e_ω) and combined in the cost function reported as follows, where the error on the rotational motion is multiplied by a factor of 100 to account for the different order of magnitude:

$$\underset{W_y}{\text{minimize}} \quad \left\|e_f(W_y)\right\|^2 + 100\left\|e_\omega(W_y)\right\|^2 \qquad (14)$$

A wider optimization loop is defined in order to find the optimal value of W_y which minimizes the cost function computed over the whole sequence of maneuvers. The optimization is performed using an interior point method[29] with a step tolerance of $1e^{-10}$. The optimal weighting factors are reported in Table 3. It can be noticed that the optimized weighting factors for the angular velocities are very similar to the initial values for both prediction strategies, therefore these weights could have been neglected in the optimization. On the other hand, the weights for specific forces differs between *oracle* and *constant*. In particular, the lowest weight for the *oracle* strategy is on f_y while the lowest for *constant* is on f_x. This difference can be related to many aspects, including the amplitude of the reference signals (maximum value of f_x higher than f_y) and the capability of each prediction strategy to obtain a feasible solution.

2.4. Dependent variables

The influence of the prediction strategy on the simulator motion is analyzed in three different aspects: (1) analysis of motion quality indicators, (2) analysis of cueing mechanism usage (3) analysis of workspace usage.

2.4.1. Motion quality indicators. A previous study[30] categorizes motion cueing errors into three types: false cues, scaling or missing cues and phase errors. Each of these cueing errors influences the motion cueing quality in a different way. In order to account for these influences when analyzing the results of the predictive MCA, it is necessary to identify some metrics to quantify the effects of each error.

Shape and scaling errors have been addressed in previous studies,[31,32] where scaling factors were adopted for the MCA and used to separate the contribution of the scaling from the shape error. In another study,[33] a more general approach was introduced based on signal correlation to analyze the error introduced only by the signals' shape. The detection threshold of phase errors introduced by the MCA have been also studied[34] and in particular for pitch and yaw motion a phase error threshold of 22 deg/s was identified.[35] A complete knowledge of these phase error thresholds for every motion channels would give the possibility to evaluate what is the maximum acceptable signal delay that will not be perceived. Unfortunately, these values are not yet known.

In a more recent article,[36] dedicated indicators for motion signal correlation, scaling and delay were defined. These indicators have been proven to correlate well with the subjective cueing quality measured in a human-in-the-loop experiment and they will be considered here to study the impact of the prediction strategy on motion cueing quality. The indicators have been slightly modified with respect to their original definition[36] and are described in detail in the following paragraphs.

Correlation coefficient (CC). This measures the signals' linear correlation. It provides a measure of similarity for the shape of the signal resulting from the MCA with

respect to the reference signal. The CC is defined as the maximum value of cross-correlation between the motion resulting from the MCA and the reference motion over all delays. For normalization purposes it is divided by the maximum auto-correlation of the reference signal and therefore it is defined in the range $[0, +1]$, where, 1 represents a perfect correlation and 0 represents no correlation. The CC is computed for the longitudinal and lateral accelerations as well as for the yaw rate, as these are the only motion channels with significant signal power in car driving maneuvers. The other motion channels mainly contain parasitic motion, due to for example tilt coordination. In the latter case, only very poor correlation is expected.

Delay indicator (DI). This indicator measures the delay between the reference signal and the signal resulting from the MCA. The indicator's value is obtained by computing the signal cross-correlation and extracting the value of signal delay that maximizes the cross-correlation. This delay is identified as DI and it is defined in the range $[0, +\infty]$. Also in this case, the indicator is used only for longitudinal and lateral accelerations, as well as for the yaw rate. Since the other motion channels do not have significant signal power, the correlation with the reference signal is not meaningful. As mentioned above, for the yaw rate, the phase error detection threshold is known and equal to 22 deg.[35] For each maneuver where the yaw rate is significant, the phase error threshold is divided by the maximum significant frequency content of each maneuver to compute the value of DI that corresponds to the phase error detection threshold. This value of DI represents the maximum signal delay that can not be perceived.

Absolute difference (AD). This indicator represents the error between the reference signal and the result of the MCA. It is defined as the area of the error signal divided by the area of the reference signal. This definition is adopted for the analysis of the longitudinal and lateral accelerations and for the yaw rate. For the analysis of pitch and roll rate, the AD is defined as the area of the absolute rate above the angular velocity perception threshold of 3 deg/s.[19] With this modification, the AD differs from 0 only if the pitch and roll rate passes the perception threshold, assuming that below that value, the motion will not be perceived.

2.4.2. Motion cueing mechanisms. The analysis of the indicators gives a very important and quantifiable measurement of motion cueing quality. Similarly to a previous study,[15] an analysis of motion cueing mechanisms provides insight to understand how the cueing quality is affected by the prediction strategy. The motion cueing mechanisms that will be analyzed in this study are presented below.

Tilt coordination. This technique is often used to reproduce sustained linear acceleration with limited workspace motion simulators. The principle is to tilt the simulator in order to use a component of the gravitational acceleration to reproduce longitudinal or lateral acceleration. This mechanism is not explicitly included in the predictive MCA, but it could still be adopted as a result of the optimization.

Prepositioning. This motion cueing mechanism is intended to maximize the simulator motion in a certain direction. The simulator moves towards the extreme of the available workspace to make use of the full motion envelope in the direction needed to reproduce accurately a certain maneuver.

Velocity buffering. This mechanism can be interpreted as the equivalent of prepositioning in velocity and it has been first identified in previous studies.[15] The simulator is moved at a certain velocity in opposite direction with respect to the one needed. At the same time the perceived motion is compensated by tilt coordination, which compensates for the acceleration that is used to generate the linear velocity. When the maneuver begins, the simulator is already moving and can be accelerated in the opposite direction for a longer time.

2.4.3. Workspace usage. A crucial limitation for motion simulators is the limited workspace available. The predictive MCA offers the possibility to include the system's constraints in the optimization problem and therefore it makes optimal usage of the available workspace. When changing the adopted prediction strategy, a different motion cueing quality is expected, together with a different usage of the simulator workspace. To determine whether the differences in motion cueing quality between prediction strategies are related to a more effective usage of simulator workspace, a dedicated analysis will be performed. In particular, the use of the actuators' length and motion envelope will be analyzed and compared.

The length of each actuator is computed for the full sequence of maneuvers. In order to analyze how the prediction strategy makes use of the actuators' length, the interquartile range is used. This quantity is normally adopted in statistics as a measure of variability and it is computed as the difference between the 75th and 25th percentiles.[37] In this study it will be assumed that a higher interquartile range would represent a wider use of the full actuator length and therefore a more effective usage of the simulator workspace.

Another aspect to notice is the use of the motion system workspace. In this study, the motion obtained for the full sequence of maneuvers with the considered prediction strategies will be analyzed separately for displacement and orientation coordinates. For the analysis of the linear displacement, the sequence of x-y-z coordinates can be visualized as a set of points in the Euclidean space. The convex hull of the sets of points obtained by each prediction strategies is computed and its volume calculated. The

obtained volumes can be compared with each other and with the complete position workspace, which is the *x-y-z* space that can be reached with every possible orientation of the motion system. A similar analysis is performed for the orientation coordinates. The roll-pitch-yaw coordinates obtained by each prediction strategy for the entire sequence of maneuvers is used to compute the convex hull. The volumes computed are again compared with each other and to the complete orientation workspace, which is the roll-pitch-yaw space that can be reached with every possible position of the motion system. In this analysis it is inferred that a higher volume of the computed convex hull indicates a larger usage of the simulator workspace.

3. Results

To compare the results obtained by the MCA with different prediction strategies, the motion quality indicators are computed and analyzed in Section 3.1. The use of different motion cueing mechanisms is presented in Section 3.2. Finally, the influence of the adopted prediction strategy on simulator workspace usage is shown in Section 3.3.

3.1. Motion quality indicators

The first analysis of the resulting simulator motion depending on the adopted prediction strategy is carried out using the indicators defined in Section 2.4.1. To clarify the analysis, the maneuvers involving similar dynamics are grouped together in three sets defined as follows:

- Longitudinal dynamics: acceleration (A) and braking (B)
- Lateral dynamics: constant turn (CT) and double lane change (DLC)
- Combined longitudinal/lateral dynamics: braking while entering the turn and accelerating while exiting the turn (BCTA).

For each maneuver set, the most relevant motion channels are considered for the calculation of the indicators.

3.1.1. Longitudinal dynamics. For the longitudinal dynamic maneuvers, the most relevant motion channels are longitudinal acceleration and pitch rate.

The results for the acceleration maneuver are shown in Figure 1. The longitudinal acceleration obtained with the *oracle* strategy is very similar to the vehicle motion, while the *constant* strategy fails to reproduce the sustained acceleration at the beginning of the maneuver resulting in a missing cue, and at the end of the maneuver providing a false acceleration cue. The CC indicator reflects the differences in the signal shape. The CC is 0.95 for the *oracle* strategy while it is 0.87 for the *constant*. The distorted acceleration signal obtained with the *constant* strategy also results in a delayed cue. In fact, the obtained DI value for the *constant* strategy is 0.86 seconds, while the DI for the *oracle* is 0.11 seconds. In terms of absolute difference, the acceleration obtained with the *oracle* is very close to the reference motion and therefore the AD is 0.10. For the *constant* strategy, due to the different shape of the signal, the difference with the reference is higher, resulting in a value of AD of 0.33. Regarding the pitch rate, the *constant* strategy keeps the resulting signal at zero until the beginning of the maneuvers, then the angular velocity rapidly increases above the perception threshold. The *oracle* strategy, knowing the future reference in advance, starts using the angular velocity before the beginning of the maneuvers, resulting in a smoother signal which barely passes the perception threshold. The quantification of this effect is provided by the AD indicator, which is 0.17 for the *oracle* strategy and 1.56 for the *constant* strategy.

Similar results for the braking maneuver are shown in Figure 2. This maneuver is more aggressive than the acceleration and therefore the differences between the two strategies are more evident. The shape of the acceleration signal for the *oracle* still follows the reference motion, with only a small reduction of motion amplitude. The indicators computed for the *oracle* reflect the motion results, with CC of 0.92, DI of 0.10 seconds and AD of 0.18. For the *constant*, the resulting motion differs from the reference. The signal shape is distorted, resulting again in false and missing cues, with an overall delayed acceleration cue. The results of the indicators for the *constant* strategy confirms the analysis of the motion signal, with CC of 0.77, DI of 1.03 seconds and a value of AD of 0.33. For the pitch rate, the signal obtained by the *oracle* strategy is again smooth but in this case it passes the perception threshold. The *constant* strategy results in a signal that is above the perception threshold for less time than the *oracle*, but with higher amplitude. The results obtained for the AD are the highest of all maneuvers, with a value of 1.73 for the *oracle* strategy and 2.66 for the *constant* strategy.

3.1.2. Lateral dynamics. For the lateral dynamic maneuvers, lateral acceleration is the most relevant motion channel, together with the roll rate and yaw rate.

The results obtained for the CT maneuver are shown in Figure 3. The lateral acceleration obtained by both prediction strategies follows the reference motion quite well, with an evident difference only in the timing of the signals. In fact, the motion obtained with the *oracle* strategy starts and ends together with the reference, while the *constant* strategy results in a delayed acceleration cue. The analysis of the motion signals finds correspondence in the indicators results, where the main difference between indicators for the lateral acceleration is obtained for the DI, which is

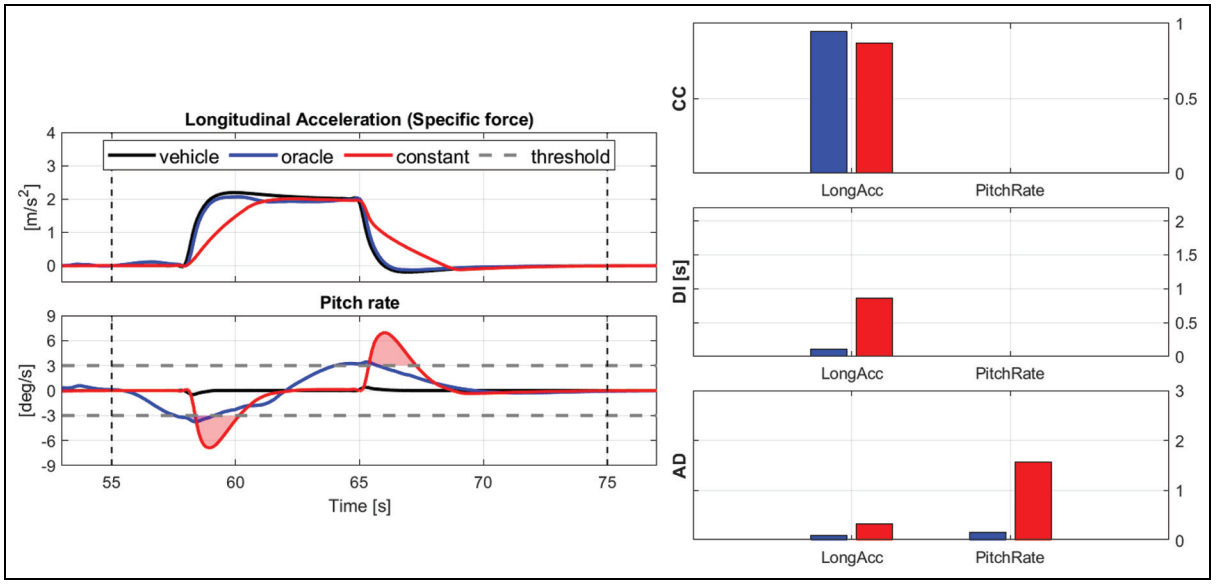

Figure 1. Resulting motion, and corresponding motion quality indicators, for the acceleration maneuver (A). The results are shown compared with the vehicle motion. Also the rotational velocity perception threshold of 3 deg/s is represented for reference.

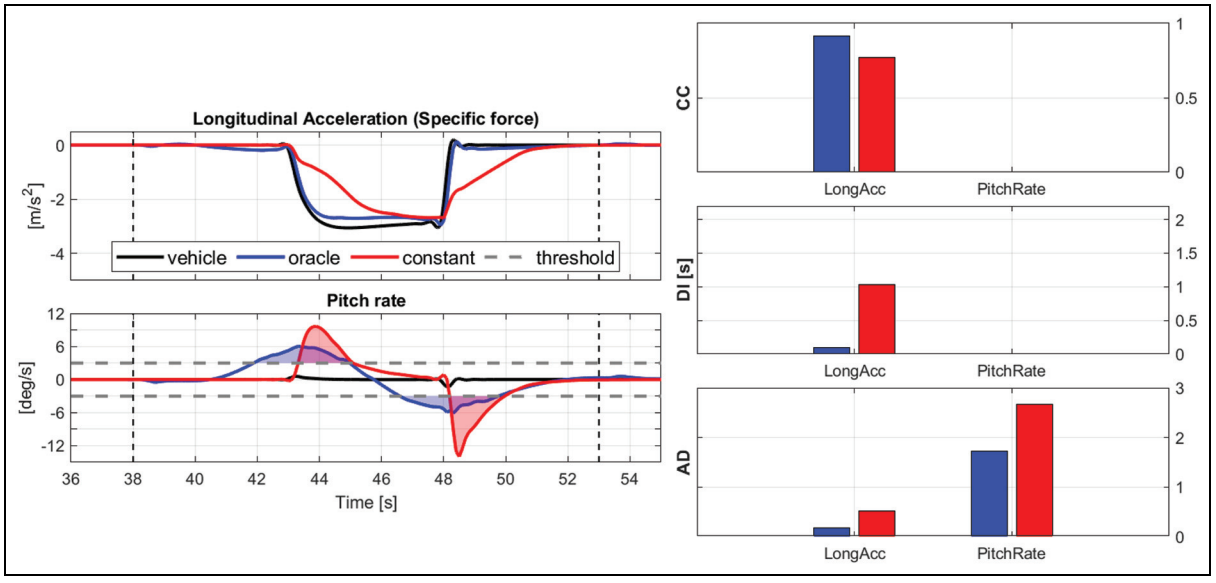

Figure 2. Resulting motion, and corresponding motion quality indicators, for the braking maneuver (B). The results are shown compared with the vehicle motion. Also the rotational velocity perception threshold of 3 deg/s is represented for reference.

0.05 seconds for the *oracle* strategy and 0.87 seconds for the *constant* strategy. The results for the correlation and absolute difference indicators do not show major differences between the prediction strategies, with CC values of 0.90 and 0.95, and AD of 0.13 and 0.17 for the *oracle* and the *constant* strategy respectively. For the roll rate, the motion signal obtained with the *oracle* strategy is always below the perception threshold, consequently the AD is 0. Oppositely, the roll rate resulting from the *constant* strategy exceeds the perception threshold, with an AD value of 0.42. Regarding the yaw rate, both the *oracle* and *constant* strategies fail to reproduce the amplitude of the reference motion signal, resulting in low values of CC and high values of AD. On the other hand, the shape of the signal can still be compared with the reference. The yaw rate obtained with the *oracle* strategy starts by going in the opposite direction but overall it has a shape very similar to the reference with only a small delay. The yaw rate resulting from the *constant* strategy is initially better than the one of the *oracle*, but at 15 seconds, changes direction and the signal

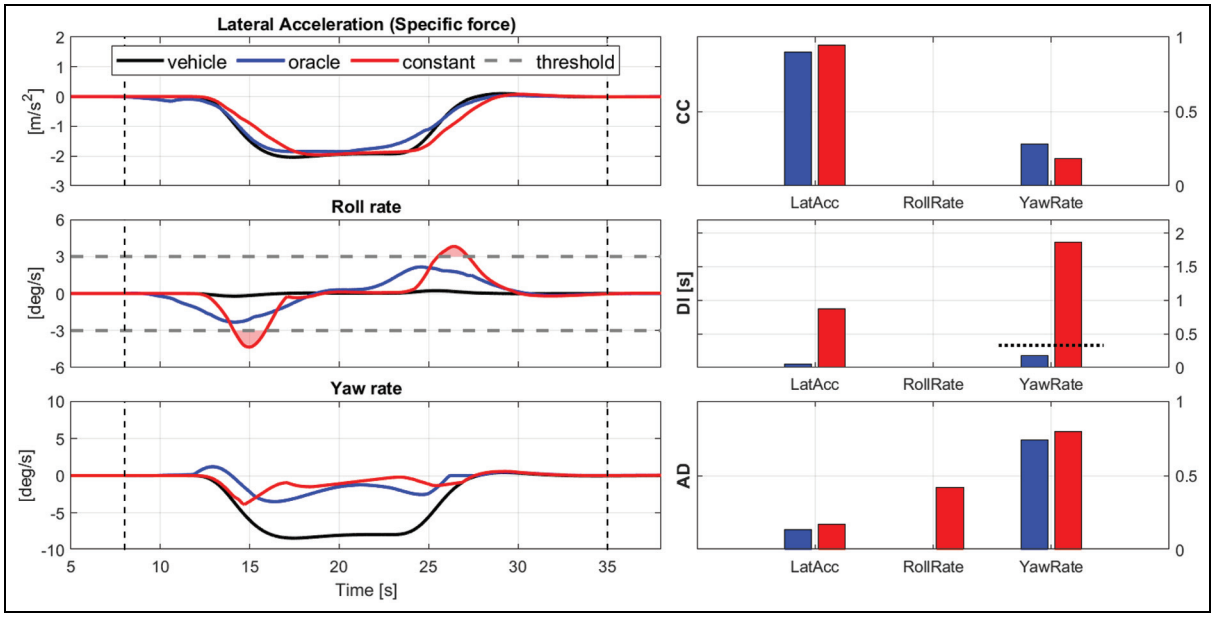

Figure 3. Resulting motion, and corresponding motion quality indicators, for the constant turn maneuver CT. The results are shown compared with the vehicle motion. Also the rotational velocity perception threshold of 3 deg/s is represented for reference. CT: constant turn.

goes almost to 0. This is reflected in the CC and DI indicators, where the CC is 0.28 for the *oracle* and 0.18 for the *constant* strategy, and the signal delay is 0.17 seconds for the *oracle* and 1.86 seconds for the *constant*. Together with the results of DI, also the delay threshold at 0.33 seconds is plotted, this value represents the maximum delay that cannot be perceived given the 22 deg of phase error threshold and the frequency content of the reference signal.

The results for the DLC maneuver are shown in Figure 4. The lateral acceleration signal obtained with the *oracle* strategy is very similar to the reference, with only a small reduction in signal amplitude. The acceleration signal obtained with the *constant* strategy has a different shape than the reference, with reduced amplitude and a delay that increases during the maneuver. Also in this case, the results of the indicators reflect the outcome of the analysis. The CC is 0.82 for the *oracle* and 0.69 for the *constant* strategy, the DI is 0.11 seconds for the *oracle* and 0.64 seconds for the *constant* strategy and finally the AD is 0.25 for the *oracle* against 0.58 for the *constant* strategy. For the roll rate, the signal computed with the *oracle* strategy is always below the perception threshold with a consequent AD value of zero, while the *constant* strategy passes the perception threshold with an AD value of 0.36. Looking at the yaw rate, the results obtained with the *oracle* is very similar to the reference motion, with a small deviation before the beginning of the maneuver and a slight delay. On the contrary, the *constant* strategy fails to reproduce the reference motion, providing a yaw rate signal which only partially reproduces the original motion. The indicators computed for the *oracle* strategy reflect the analysis of the motion, with a CC of 0.96 and a DI of 0.12 seconds. The computed DI is also below the delay threshold of 0.22 seconds. The resulting DI value for the *constant* strategy is equal to 0.03 which is even lower than the DI obtained with the *oracle*, this is most likely due to the very different signal shape which invalidates the result. The AD obtained is equal to 0.23 for the *oracle* and 0.70 for the *constant* strategy.

3.1.3. Longitudinal/lateral dynamics. For the analysis of the indicators of the combined dynamic maneuver, the motion channels for both longitudinal and lateral dynamics are considered.

The results obtained for the combined dynamic maneuver are shown in Figure 5. The longitudinal acceleration obtained with the *oracle* strategy is again very similar to the reference motion, the signal shape corresponds, with a short delay and a small difference in amplitude. The corresponding indicator values reflect the analysis with CC of 0.94, DI of 0.11 seconds and AD of 0.13. On the contrary, the longitudinal acceleration resulting from the *constant* strategy differs from the reference motion. The signal shape is distorted, with alternating missing and false cues and an overall delayed signal. The results given by the indicators are representative of these differences, with CC of 0.86, a DI of 0.82 seconds and AD of 0.44. For the lateral acceleration the differences between the motion obtained by the two prediction strategies is less evident

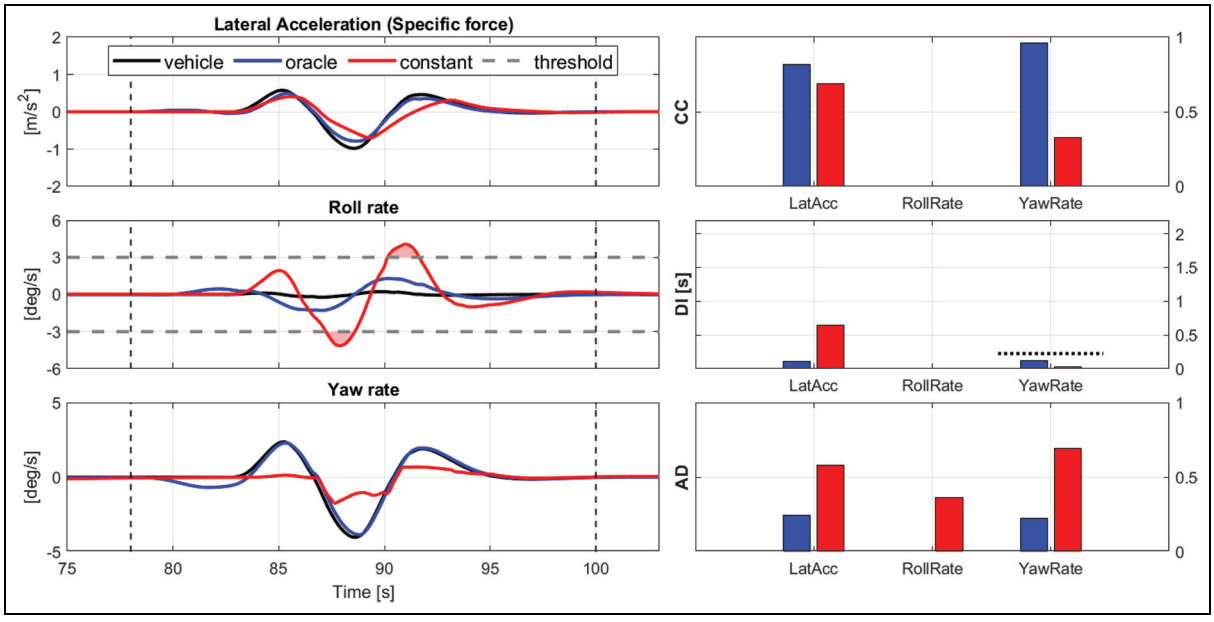

Figure 4. Resulting motion, and corresponding motion quality indicators, for the double lane change maneuver (DLC). The results are shown compared with the vehicle motion. Also the rotational velocity perception threshold of 3 deg/s is represented for reference.
DLC: double lane change.

but still present. Regarding the shape of the signals, the best result is obtained with the *constant* strategy, which contrary to the *oracle*, is able to reproduce also the peak of acceleration between 120 and 125 seconds. The CC obtained with the *constant* strategy is 0.95, while for the *oracle* is 0.89. On the other hand, the lateral acceleration motion obtained with the *constant* is delayed with respect to the reference, resulting in a DI of 0.80 seconds. In comparison, the DI computed for the *oracle* is 0.18 seconds. The absolute difference for the lateral acceleration motion is comparable for the two prediction strategies, with a value of AD of 0.15 for the *oracle* and 0.22 for the *constant* strategy. For the pitch and roll rate, the motion obtained with the *oracle* strategy is mostly smooth and always below the perception threshold and consequently the AD is in both cases equal to 0. In contrast with the *oracle*, the motion signals obtained with the *constant* strategy is less smooth and passes the perception threshold for both roll and pitch rate, with AD of 0.05 for the roll rate and 0.28 for the pitch rate. For the yaw rate, the resulting motion signals are both different from the reference motion in terms of shape and amplitude, but the signal obtained with the *oracle* strategy is better synchronized with the reference. The indicator results for correlation and absolute difference are very similar for both strategies, with CC of 0.36 and 0.37 and AD of 0.64 and 0.65 for the *oracle* and *constant* strategy respectively. The only clear difference in the indicator results is obtained for the DI, which is 0.20 seconds for the *oracle* and 2.04 seconds for the *constant* strategy. Also in this case the delay threshold is computed, the result is 0.31 seconds, which is higher than the DI obtained with the *oracle* strategy.

3.2. Motion cueing mechanisms

Tilt coordination is used in all maneuvers by both prediction strategies. In Figure 6, both effects of tilt coordination and velocity buffering can be seen. The usage of tilt coordination from both prediction strategies is evident from the analysis of the components of the longitudinal acceleration. In fact, only the linear component of the acceleration would not be sufficient to reproduce the sustained acceleration, therefore the gravitational component is used, tilting the motion system to use a component of the gravitational acceleration.

Also the effect of velocity buffering can be seen in Figure 6, in particular between 40 and 45 seconds and between 55 and 60 seconds. The *oracle* strategy starts accelerating the platform in the opposite direction, while compensating with tilt coordination. The *constant* does not make use of velocity buffering as it starts to tilt the motion platform only when the acceleration begins.

An example of prepositioning can be seen in Figure 7, where the lateral displacement of the motion system is shown together with the resulting lateral acceleration for each prediction strategy. A few seconds before the maneuver, the *oracle* strategy moves on one extreme of the available workspace, making possible the use of a longer

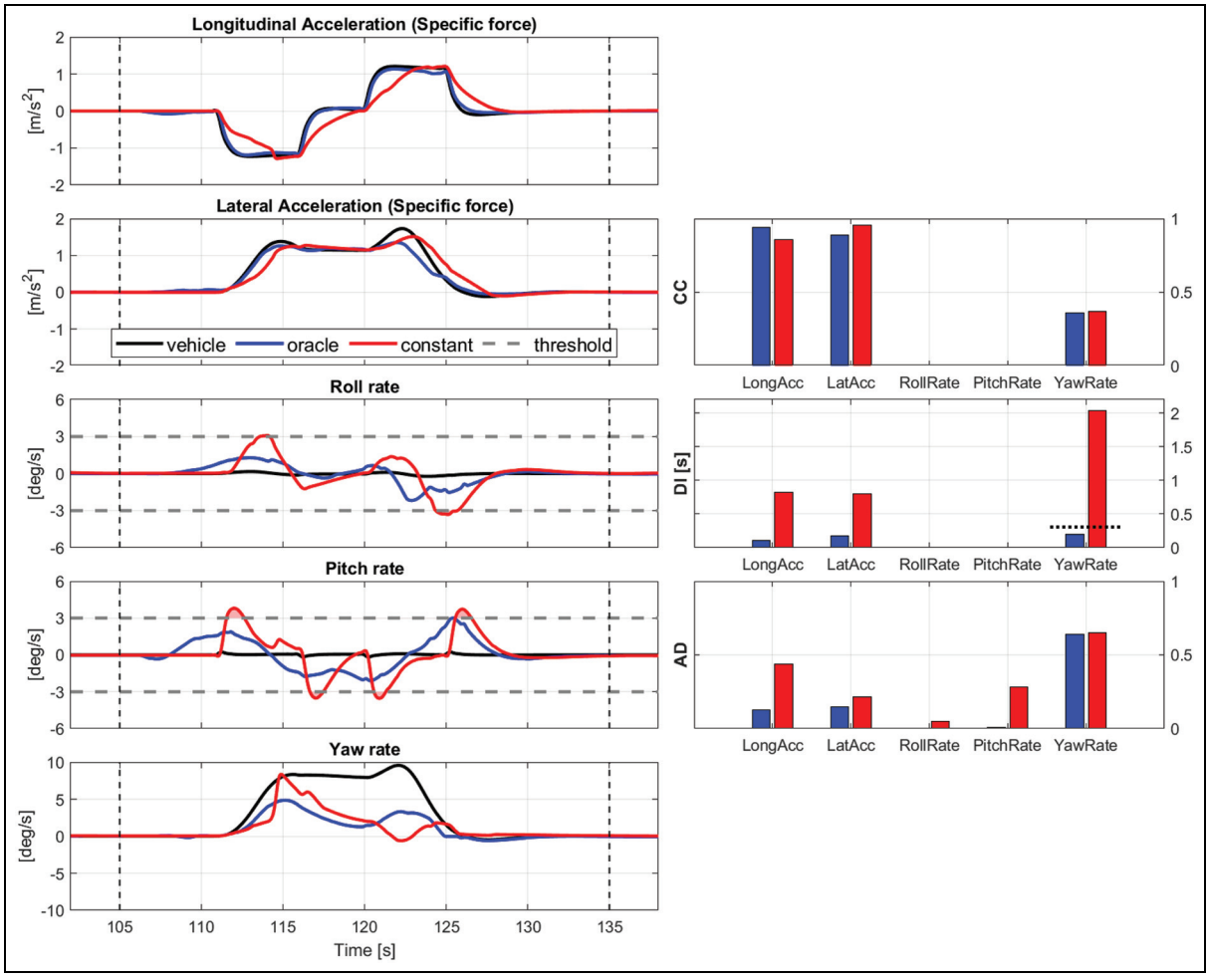

Figure 5. Resulting motion, and corresponding motion quality indicators, for the combined dynamic maneuver BCTA. The results are shown compared with the vehicle motion. Also the rotational velocity perception threshold of 3 deg/s is represented for reference.
BCTA: braking while entering the turn and accelerating while exiting the turn.

excursion to reproduce the lateral acceleration. The *constant* strategy does not show similar behavior, by starting the simulator motion at the start of the maneuver.

3.3. Workspace usage

The actuators' length is computed for the entire sequence of maneuvers and for the two prediction strategies. The length of each actuator is then normalized between 0 and 1 and the interquartile range is computed. The results are shown in Figure 8, where it can be seen that the interquartile range is always larger for the *oracle* strategy compared to the *constant* strategy and therefore it can be inferred that the *oracle* makes more use of the actuators' length.

Regarding the usage of the motion platform position workspace, the results are shown in Figure 9 for translations and Figure 10 for rotations, where the motion envelope for the reproduction of the entire sequence of maneuvers is shown for both prediction strategies. For translations, the volume of the convex hull of the motion envelope used by the *constant* is 0.0451 m^3 and the volume used by the *oracle* is 0.0642 m^3, which is 42.4% larger. In addition to this, it can be noticed that the *oracle* uses the workspace also in proximity of the physical system's limitation. From the top view of Figure 9 it can be noticed that the maximum longitudinal position reached by the *oracle* is very close to the position workspace limit. This point is reached during the braking maneuver, where a large longitudinal displacement is needed to reproduce the reference acceleration. Similarly, the results obtained for the orientation workspace are shown in Figure 10. The volume of the convex hull of the motion envelope used by the *constant* is 5.54e6 deg^3 and the volume used by the *oracle* is 6.17e6 deg^3, which is 11.4% larger.

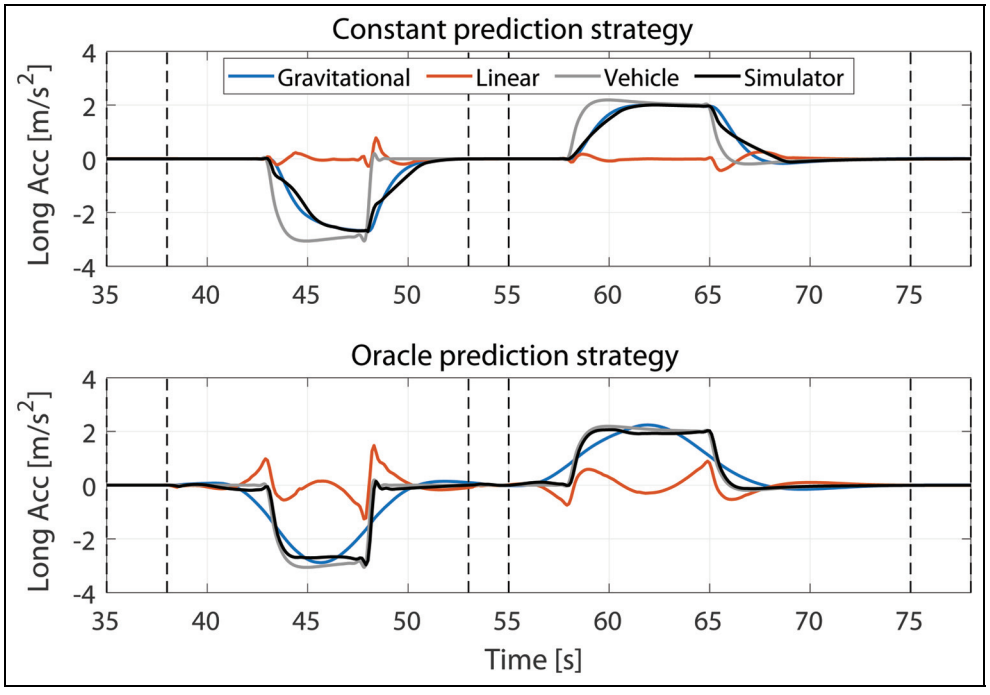

Figure 6. Different contributions to linear acceleration reproduction for the *oracle* and *constant* prediction strategy in longitudinal dynamic maneuvers.

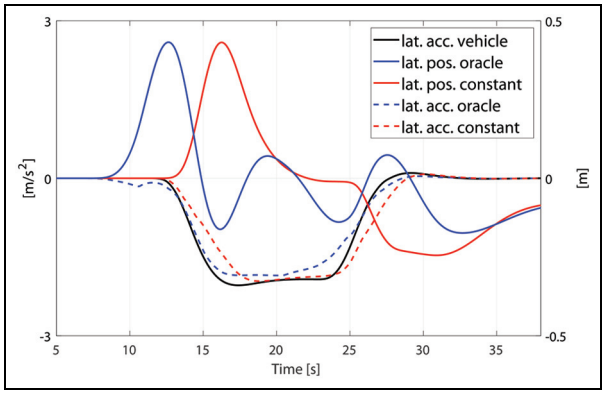

Figure 7. Comparison of simulator lateral displacement and perceived lateral acceleration during the constant turn maneuver for the *oracle* and *constant* prediction strategy.

4. Discussion

The inspection of actual response curves and the corresponding motion quality indicators shows that the indicators are able to qualify and quantify the differences between the reference motion and the motion obtained with the considered prediction strategies. From the results it emerges that several indicators are useful to understand one particular difference between the signals (i.e., shape difference, delay or absolute difference) but only the combined analysis of the indicators provides a complete understanding of the motion resulting from a particular prediction strategy.

The *oracle* strategy achieves higher motion cueing quality than the *constant* strategy by starting the simulator motion before the beginning of the maneuvers, allowing the use of prepositioning and velocity buffering, in addition to tilt coordination, which is the only motion cueing mechanism adopted by the *constant* strategy. The combined use of multiple motion cueing mechanisms adopted by the *oracle* leads to a larger interquartile range for the actuators and therefore to a better use of the simulator workspace, especially when most needed. For example, in the braking maneuver, when the longitudinal acceleration reaches its maximum, the *oracle* strategy results in a simulator motion very close to the maximum longitudinal displacement of the hexapod. It is important to notice that the motion cueing mechanisms are not direct functionalities of the predictive MCA but rather the results of the optimization and they provide better results when the future prediction is perfectly accurate. When the future prediction is incorrect, the quality of the motion cueing could be reduced by a misuse of the motion cueing mechanisms resulting from the attemp of the predictive MCA to reproduce an incorrect reference.

From the results obtained for the workspace usage, it can also be inferred that to achieve the same motion cueing quality performances, the *oracle* requires a smaller motion

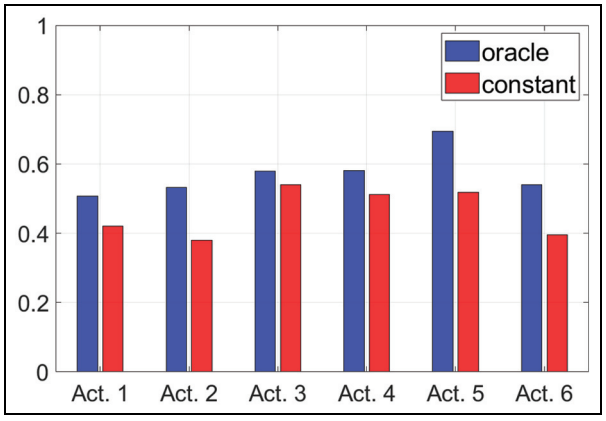

Figure 8. Interquartile range of the normalized actuators' length for all the maneuvers. Comparison between the adopted prediction strategies.

system workspace than the *constant*. Or, that the *constant* strategy requires a larger workspace to achieve the same motion cueing quality that can be obtained with the *oracle* strategy.

Moreover, from the analysis of the simulator motion, it can be noticed that the *constant* strategy results are less smooth, with higher linear jerk and angular acceleration values. Previous studies[38,39] found that this can reduce the quality of perceived motion, which is another aspect that underlines the lower performances of the *constant* with respect to the *oracle* strategy.

The analysis of the maneuvers divided in longitudinal, lateral and combined dynamics shows that the differences in motion cueing quality between *oracle* and *constant* are more evident especially for longitudinal and combined dynamic maneuvers. In particular for longitudinal dynamic maneuvers, the analysis shows large improvement with a more accurate prediction strategy knowing future motion. Nevertheless, the *oracle* strategy cannot be used for DIL simulations, while the *constant* strategy, with its suboptimal results, can be used for simulating active driving. The results indicate that it is worthwhile to invest in a better prediction than the *constant* and this could be done by

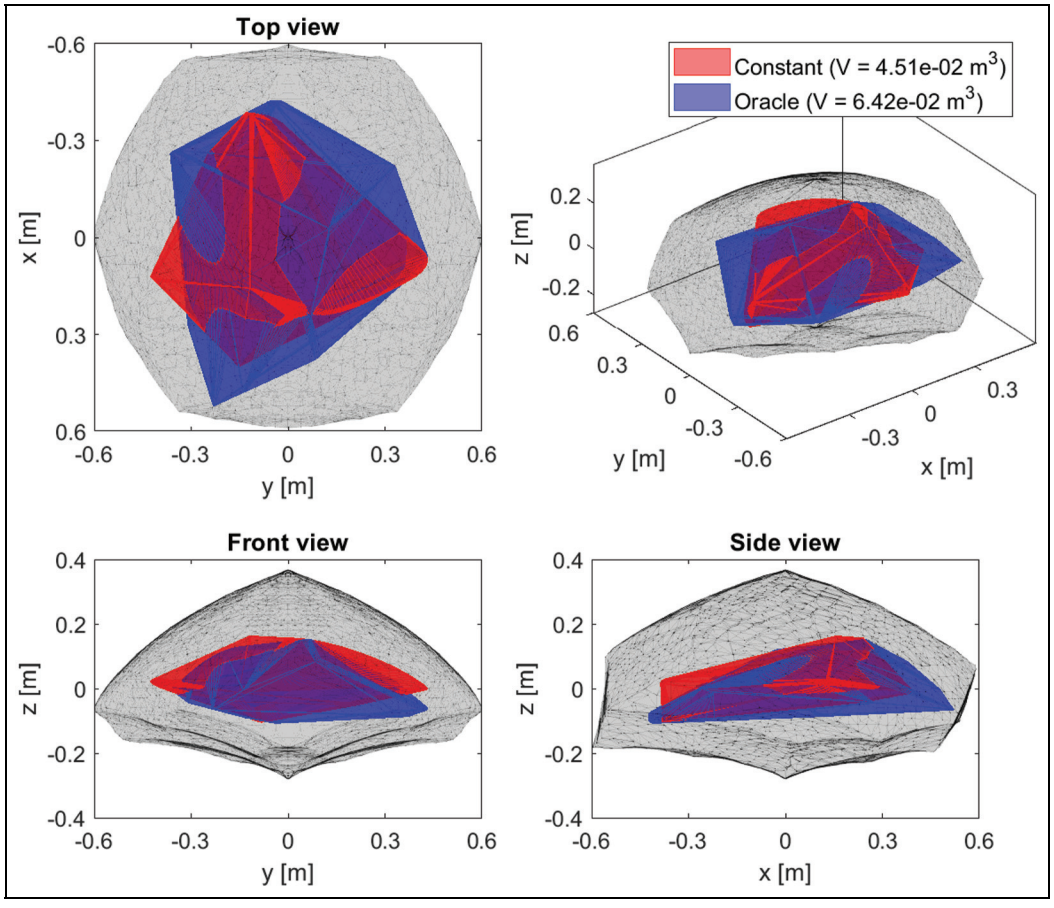

Figure 9. Simulator position workspace comparison between *oracle* and *constant* prediction strategy. The motion envelope is computed considering *x*-*y*-*z* coordinates. The bigger area represented in light grey is the complete motion platform position workspace considering all reachable orientation.

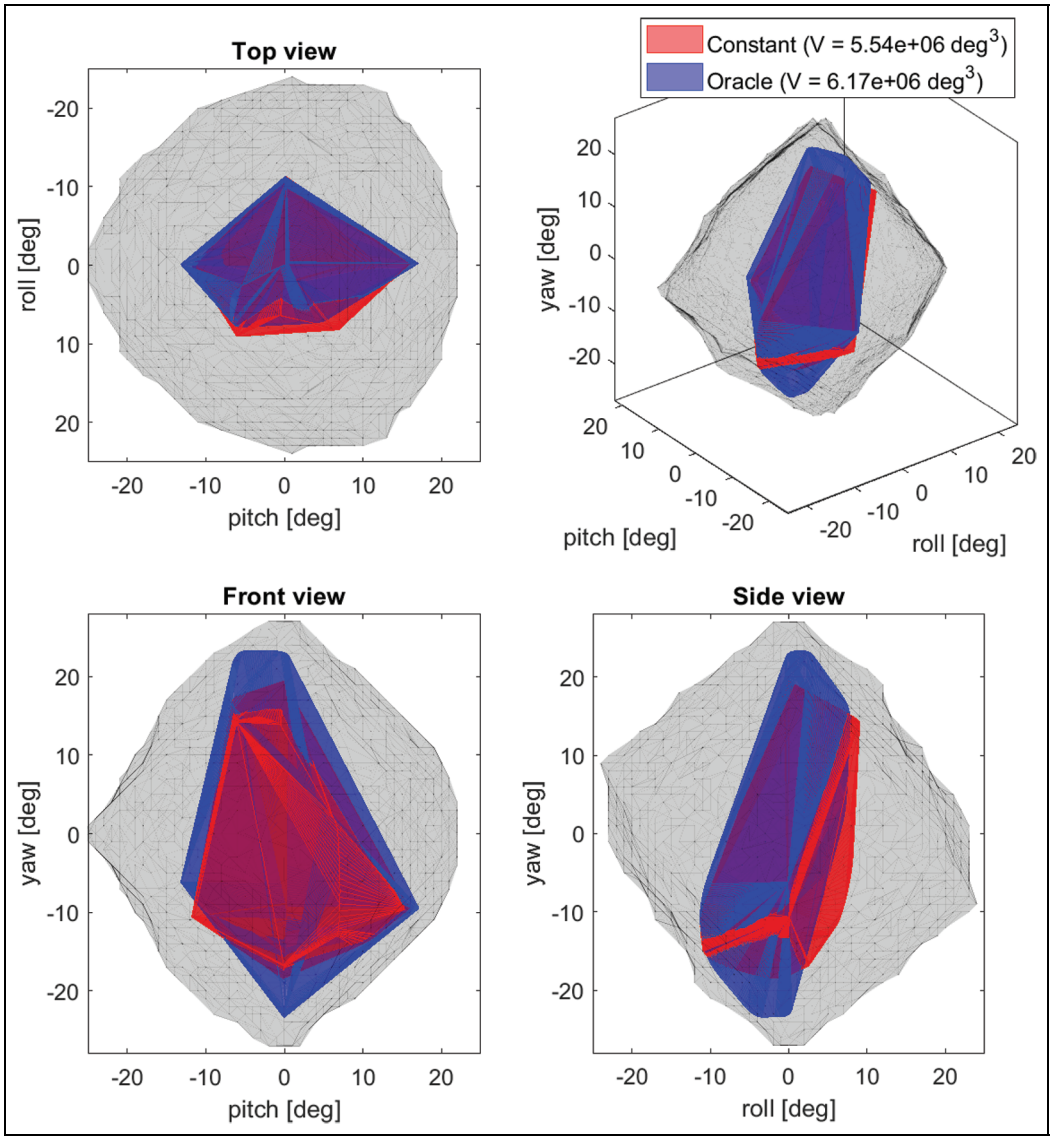

Figure 10. Simulator orientation workspace comparison between the *oracle* and *constant* prediction strategy. The motion envelope is computed considering roll-pitch-yaw coordinates. The bigger area represented in light grey is the complete motion platform orientation workspace considering all reachable position.

using information about the road and traffic, such as traffic signs/lights and/or velocity of leading vehicles. The information could be used to predict if the driver will accelerate or brake the vehicle. Similarly, for the lateral dynamics, information about the future road profile can be used to foresee turning maneuvers. These approaches could be combined with a simplified vehicle model to predict longitudinal and lateral accelerations. Such a prediction strategy would result in improved motion cueing quality performances and still be usable in DIL simulations.

Finally, the objective evaluation carried out in this study is based on objective metrics that have been shown to highly correlate with subjective evaluation and therefore, the results of objective and subjective evaluations are expected to correspond. Nevertheless, it is useful to conduct a human-in-the-loop experiment to identify which indicator weighs most for the overall perceived motion quality and what is the difference between indicator values which is large enough for humans to detect the quality difference. A suitable method to adopt here could be the continuous rating method,[40] where the subjects of a passive driving experiment continuously provide a feedback of the mismatch between visual and motion.

5. Conclusions

In this study, the effects of two prediction strategies on optimization-based MCA have been analyzed. The first strategy, *oracle*, assumes perfect knowledge of future vehicle motion, it cannot be used for DIL simulations and it is considered as a reference to evaluate the best motion cueing quality that can be achieved. The second strategy, *constant*, ignores changes in the future reference and assumes a constant reference equal to last vehicle status. The objective analysis carried out aimed to qualify and quantify the effects of the prediction strategies by means of dedicated metrics. Motion cueing quality indicators have been defined to quantify correlation, delay and absolute difference of the simulator motion with respect to the reference vehicle motion. An analysis of the adopted motion cueing mechanisms has been performed together with a study on the usage of the motion system workspace. As expected, the *oracle* outperforms the *constant* strategy, being able to coordinate the usage of multiple motion cueing mechanisms and manage the use of the limited workspace to obtain better motion cueing quality performances. The combined analysis of multiple indicators confirms the differences in performance and provides the metrics to quantify these differences. From the indicator results, the larger performance difference is obtained for longitudinal dynamic maneuvers, providing an indication of what should be improved in the future design of advanced prediction strategies for optimization-based MCAs.

Acknowledgements

The authors acknowledge the Max Planck Institute for Biological Cybernetics, the researchers and the technicians who were involved in this study. In particular, Maria Lächele, Joachim Tesch and Daniel Diers are kindly acknowledged for their technical support. Mikhail Katliar and Ksander de Winkel are also acknowledged for the helpful discussions and suggestions.

Funding

The research leading to these results has received fundings from the People Programme (Marie Curie Actions) of the European Union's Seventh Framework Programme FP7 2007-2013 under REA grant agreement n. 608092, 'MOTORIST' (www.motorist-ptw.eu).

ORCID iD

Marco Grottoli https://orcid.org/0000-0002-7542-9763

References

1. Schmidt SF and Conrad B. Motion drive signals for piloted flight simulators. Technical report, NASA, Washington, 1970.
2. Reid LD and Nahon MA. Flight simulator motion-base drive algorithms: Part 1: developing and testing the equations. Technical report, University of Toronto Institute for Aerospace Studies, 1985.
3. Reid LD and Nahon MA. Flight simulator motion-base drive algorithms: Part 2: selecting the system parameters. Technical report, University of Toronto Institute for Aerospace Studies, 1986.
4. Grant PR and Reid LD. PROTEST: An expert system for tuning simulator washout filters. *J Aircraft* 1997; 34: 152–159.
5. Casas S, Coma I, Portalés C, et al. Towards a simulation-based tuning of motion cueing algorithms. *Sim Model Pract Th* 2016; 67: 137–154.
6. Casas S, Portalés C, Morillo P, et al. A particle swarm approach for tuning washout algorithms in vehicle simulators. *Appl Soft Comput* 2018; 68: 125–135.
7. Dagdelen M, Reymond G, Kemeny A, et al. MPC-based motion cueing algorithm: development and application to the ULTIMATE driving simulator. In: *Driving simulation conference*, September 2004. pp. 221–233.
8. Fang Z and Kemeny A. An efficient model predictive control-based motion cueing algorithm for the driving simulator. *Simulation* 2016; 92: 1025–1033.
9. Baseggio M, Beghi A, Bruschetta M, et al. An MPC approach to the design of motion cueing algorithms for driving simulators. In: *2011 14th international IEEE conference on intelligent transportation systems (ITSC)*, Washington, D.C, 5–7 October 2011, pp. 692–697. Piscataway, NJ: IEEE.
10. Garrett NJI and Best MC. Model predictive driving simulator motion cueing algorithm with actuator-based constraints. *Vehicle Sys Dyn* 2013; 51: 1151–1172.
11. Rawlings JB and Mayne DQ. *Model predictive control: theory and design*. Madison, WI: Nob Hill Publishing, 2009.
12. Maciejowski JM. *Predictive control with constraints*. Harlow: Pearson education, 2002.
13. Wang L. *Model predictive control system design and implementation using MATLAB®*. Advances in industrial control, London: Springer London, 2009.
14. Camacho EF and Bordons C. *Model predictive control*. Advanced textbooks in control and signal processing. London: Springer London, 2007.
15. Cleij D, Venrooij J, Pretto P, et al. Comparison between filter- and optimization-based motion cueing algorithms for driving simulation. *Transport Res Part F: Traffic Psychol Behav* 2017. Article In Press.
16. Bruschetta M, Cenedese C and Beghi A. A real-time, MPC-based motion cueing algorithm with look-ahead and driver characterization. *Transport Res Part F: Traffic Psychol Behav* 2017. Article In Press
17. Mohammadi A, Asadi H, Mohamed S, et al. Future reference prediction in model predictive control based driving simulators. In: *ACRA 2016: Proceedings of the ARAA Australian conference on robotics and automation*, Queensland, 5–7 December 2016, p. 8. Brisbane, Qld.: Australian Robotics and Automation Association.
18. Reymond G and Kemeny A. Motion cueing in the renault driving simulator. *Vehicle Sys Dyn* 2000; 34: 249–259.
19. Nesti A, Masone C, Barnett-Cowan M, et al. Roll rate thresholds and perceived realism in *driving simulation*. In: *Driving simulation conference*, 6–7 September 2012, p. 6. Paris, France.

20. Nesti A, Nooij S, Losert M, et al. Roll rate perceptual thresholds in active and passive curve driving simulation. *Simulation* 2016; 92: 417–426.
21. Telban RJ and Cardullo FM. Motion cueing algorithm development: Human-centered linear and nonlinear approaches. Technical Report, ID 20050180246, 1 May 2005, NASA Technical Reports Server (NTRS).
22. Stewart D. A platform with six degrees of freedom. *Proc Inst Mech Eng 1847–1982 (vols 1–196)* 1965; 180: 371–386.
23. Salisbury IG and Limebeer DJN. Optimal motion cueing for race cars. *IEEE Trans Contr Sys Technol* 2016; 24: 200–215.
24. Diehl M, Bock HG and Schlöder JP. A real-time iteration scheme for nonlinear optimization in optimal feedback control. *SIAM J Contr Optim* 2005; 43: 1714–1736.
25. Ferreau HJ, Kirches C, Potschka A, et al. qpOASES: a parametric active-set algorithm for quadratic programming. *Math Prog Comput* 2014; 6: 327–363.
26. Katliar M, Fisher J, Frison G, et al. Nonlinear model predictive control of a cable-robot-based motion simulator. In: *The 20th world congress of the international federation of automatic control*, Toulouse, 9–14 July 2017, pp. 10249–10255.
27. Mohammadi A, Asadi H, Mohamed S, et al. Optimizing model predictive control horizons using genetic algorithm for motion cueing algorithm. *Exp Sys App* 2018; 92: 73–81.
28. Katliar M, de Winkel KN, Venrooij J, et al. Impact of MPC prediction horizon on motion cueing fidelity. In: *Driving simulation conference & exhibition 2015*. Tübingen, 16–18 September 2015. Tübingen, Germany: Max Planck Institute for Biological Cybernetics.
29. Boyd SP and Vandenberghe L. *Convex optimization*. New York, NY, USA: Cambridge University Press, 2004.
30. Grant PR and Reid LD. Motion washout filter tuning: rules and requirements. *J Aircraft* 1997; 34: 145–151.
31. Grant P, Artz B, Blommer M, et al. A paired comparison study of simulator motion drive algorithms. In: *Driving simulation conference 2002*, Paris, September 2002, pp. 1–13.
32. Fischer M and Werneke J. The new time-variant motion cueing algorithm for the DLR dynamic driving simulator. In: *Driving simulation conference 2008*, Monaco, 31 January–1 February 2008, pp. 57–67.
33. Qaisi IA and Traechtler A. Human in the loop: Optimal control of driving simulators and new motion quality criterion. In: *2012 IEEE international conference on systems, man, and cybernetics (SMC)*, Seoul, 14–17 October 2012, pp. 2235–2240. Piscataway, NJ: IEEE.
34. Grant PR and Lee PT. Motion-visual phase-error detection in a flight simulator. *J Aircraft* 2007; 44: 927–935.
35. Jonik P, Valente Pais AR, van Paassen MM, et al. Phase coherence zones in flight simulation. In: *AIAA Modeling and Simulation Technologies Conference*, Portland, OR, 8–11 August 2011, pp. 2039–2048. Reston, Virigina: American Institute of Aeronautics and Astronautics.
36. Casas S, Coma I, Riera JV, et al. Motion-cuing algorithms: characterization of users perception. *Human Fact* 2015; 57: 144–162.
37. Montgomery DC and Runger GC. *Applied statistics and probability for engineers*. 3rd ed. John Wiley & Sons, Inc., Hoboken, NJ, USA, 2003.
38. Grant PR and Haycock B. Effect of jerk and acceleration on the perception of motion strength. *J Aircraft* 2008; 45: 1190–1197.
39. Soyka F, Teufel H, Beykirch K, et al. Does jerk have to be considered in linear motion Simulation? In: *AIAA Modeling and Simulation Technologies Conference 2009*, 10–13 August 2009. Reston, Virigina: American Institute of Aeronautics and Astronautics, pp. 1381–1388.
40. Cleij D, Venrooij J, Pretto P, et al. Continuous rating of perceived visual-inertial motion incoherence during driving simulation. In: *Driving simulation conference & exhibition 2015*, Tübingen, 16–18 September 2015, pp. 16–18. Tübingen, Germany: Max Planck Institute for Biological Cybernetics.

Author biographies

Marco Grottoli obtained an MSc in Mechanical Engineering with a focus on Mechatronics and Robotics from Politecnico di Milano in 2014. He is currently enrolled in a PhD program in Biomechanical Engineering at Delft University of Technology, the Netherlands, and works as a Research Engineer in Siemens PLM Software, Belgium. He worked in the MOTORIST project with a focus on modelling and simulation techniques for motorcycle simulators and implementation and evaluation of motion cueing algorithm for motion-based simulators.

Diane Cleij received an MSc from the Technical University in Delft, the Netherlands, in the field of control and simulation at the faculty of Aerospace Engineering. After the Masters, she worked in industry for 2 years as a mechatronics designer at Alten Mechatronics and ASML. In 2014 she started a PhD at the Max Planck Institute for Biological Cybernetics, Germany. Her work focuses on investigating the relation between visual and inertial mismatch and the time varying perceived realism in motion-based simulators.

Paolo Pretto obtained an MSc in psychology and a bi-national PhD in perception, psychophysics and behavioral sciences. He worked as a team leader in the Motion Perception and Simulation research group at the Max Planck Institute for Biological Cybernetics, Germany. Currently he is the key researcher on human factors at Virtual Vehicle, Austria. His work focuses on the perception and control of self-motion in a realistically simulated environment, with emphasis on driving contexts.

Yves Lemmens has an MSc degree from the University of Brussels, Belgium and a PhD at Cranfield University, UK. He is currently a senior research manager at the Simulation and Test Solutions business segment of Siemens PLM Software. He leads research activities that focus on model, hardware and human-in-the-loop

simulation of complex mechatronic systems for automotive and aerospace applications.

Riender Happee received his MSc degree in Mechanical Engineering (1986) and PhD degree (1992) at TU Delft. He introduced biomechanical human models for impact and comfort simulation at TNO Automotive (1992–2007). He is currently at TU Delft at the Faculties of Mechanical, Maritime and Materials Engineering, and Civil Engineering and Geosciences. He investigates the human interaction with automated and manually driven vehicles, including WEpods, a national project on driverless public transport in urban conditions (https://www.gelderland.nl/wepods), HFAuto, Human Factors of Automated Driving, a European project focusing on safe user interaction with automated vehicles in highway conditions (http://hf-auto.eu), and two-wheeled vehicles (http://www.motorist-ptw.eu).

Heinrich H. Bülthoff is the Director of the Department of Human Perception, Cognition and Action at the Max Planck Institute for Biological Cybernetics, and a member of the Max Planck Society. He is Honorary Professor at the Eberhard Karls University in Tübingen, Germany, and Distinguished Professor at Korea University in Seoul, Korea. He holds a PhD degree in natural sciences. His research interests include object recognition and categorization, perception and action in virtual environments, and human–robot interaction and perception.